Experimental Testing of an Oil-Flooded Hermetic Scroll Compressor

Ian H. Bell[a,*], Eckhard A. Groll[b], James E. Braun[b], W. Travis Horton[b]

[a] *University of Liège, Department of Aerospace and Mechanical Engineering, Liège, Belgium*
[b] *Purdue University Department of Mechanical Engineering, 140 S. Martin Jischke Drive, West Lafayette, IN, 47906*

Abstract

In this work, a residential air conditioning compressor designed for vapor injection has been modified in order to inject large quantities of oil into the working chamber in order to approach an isothermal compression process. The compressor was tested with oil injection mass flow fractions of up to 45%. At an evaporating temperature of -10°C and condensing temperature of 30°C, the overall isentropic efficiency was up to 70% at the highest oil injection rate. Overall, over the testing envelope investigated, there are no significantly negative effects experienced for the compressor and the compressor isentropic efficiency and refrigerant mass flow rate improve monotonically as the oil injection rate is increased.

Keywords:
Air conditioning, Refrigeration, Flooded Compression

1. Introduction

The primary motivation for the use of liquid flooding in compressors is that it can allow for a working process that approaches isothermal compression. From simplified air conditioning cycle analysis (Bell et al., 2011), it has been shown that the benefits to cycle efficiency can be quite large for large temperature lifts with the addition of liquid flooding and regeneration. The major question raised by this work was how well hermetic scroll compressors would perform when they were flooded with oil.

The concept of liquid flooding of refrigerant compressors with a high-specific-heat liquid is not a new idea. In fact, this technique has been applied to screw compressors for some years in order to decrease leakage and control the discharge temperature of the compressor. Some experimental data is available for the flooding of screw, scroll, and spool compressors (Blaise and Dutto, 1988; Stosic et al., 1990; Hiwata, 2002; Kemp, 2010), but much of the experimental data is poorly characterized, or does not employ sufficiently high oil flooding rates. Bell (2011) has a more exhaustive survey of the experimental and modeling efforts related to liquid-flooded compression.

2. Experimental Setup

A scroll compressor was installed in a hot-gas bypass load stand for performance testing with oil injection. Figure 1 shows a schematic of the hot gas bypass stand prior to modification for oil injection testing. Refrigerant is compressed from state point 1 to state point 2 in the compressor, then throttled down to an intermediate pressure at state point 3. At state point 3, some fraction of the flow is throttled through a bypass valve to state point 6. The remaining refrigerant is condensed in the condenser to state point 4, at which point it is throttled from the intermediate pressure down to the suction pressure. This cooled two-phase refrigerant at state point 5 is then mixed with the bypass stream and enters the compressor once again. A pressure-enthalpy plot for the hot-gas bypass stand is shown in Figure 2.

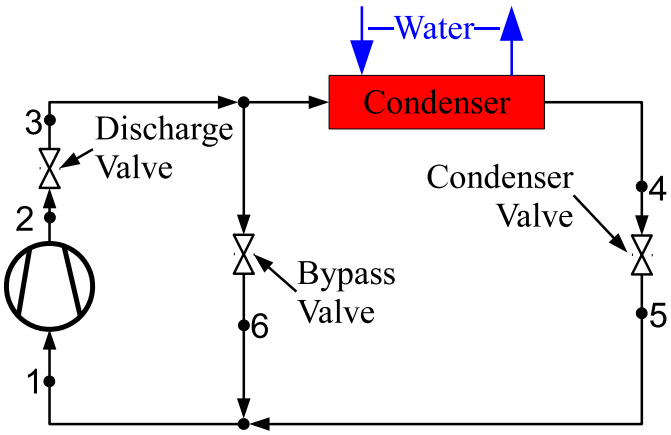

Figure 1: Simplified hot-gas bypass stand

The benefit of using the hot-gas-bypass-type load stand is that the intermediate pressure stays relatively constant at a value corresponding to a saturation temperature slightly above the condenser water inlet temperature. The exact intermediate pressure depends on the refriger-

*Corresponding Author
Email addresses: ian.bell@ulg.ac.be (Ian H. Bell), groll@purdue.edu (Eckhard A. Groll), jbraun@purdue.edu (James E. Braun), wthorton@purdue.edu (W. Travis Horton)

Nomenclature

h_1	Compressor inlet enthalpy (kJ kg^{-1})
$h_{2s,inj}$	Isentropic enthalpy for injection (kJ kg^{-1})
$\dot{m}_l$	Liquid mass flow rate (g s^{-1})
$\dot{m}_{ref}$	Refrigerant mass flow rate (g s^{-1})
ΔT_{sh}	Compressor inlet superheat (°C)
T_1	Compressor inlet temperature (°C)
T_{11}	Liquid inlet temperature (°C)
$T_{dew,s}$	Suction dewpoint temperature (°C)
$T_{dew,d}$	Discharge dewpoint temperature (°C)
$\dot{W}_{el}$	Electrical power input (kW)
$\dot{W}_i$	Isentropic power (kW)
x_l	Liquid mass flow fraction (-)
η_{oi}	Overall isentropic efficiency (-)

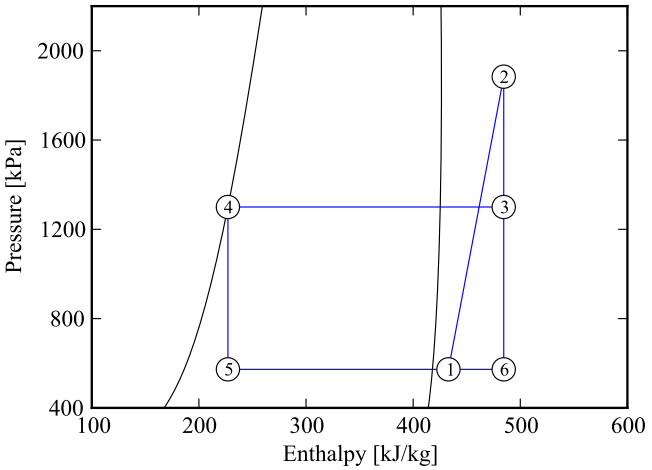

Figure 2: Pressure-enthalpy plot of bypass stand

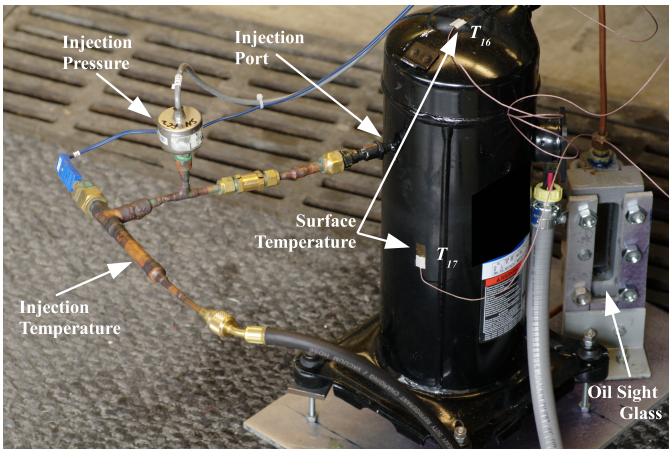

Figure 4: Photograph of compressor installed and instrumented

ant charge level and heat transfer in the condenser, but is typically on the order of 5 K above the water inlet temperature.

For the testing conducted here, a few modifications were made to the standard hot-gas-bypass configuration. Two oil loops were added to the stand - a primary oil loop as well as an oil injection loop. Figure 3 shows a schematic representation of the modified system. The primary oil separator is used to store oil for return to the sump of the compressor when the oil in the compressor is depleted. The metering valve labeled MV3 can be opened to add oil to the suction gas stream going into the compressor and refill the compressor oil sump.

The second oil separator is used to process the oil that is injected into the compressor for the purposes of achieving a more-isothermal compression process. When the oil-refrigerant vapor stream exits the compressor, the flow can be balanced between the two separators. In general, only one separator was used at a time. For the oil injection loop separator, a two-phase mixture of oil and refrigerant vapor enter the separator, and essentially pure vapor exits out the top of the separator. Oil with some amount of dissolved refrigerant then exits the separator from a dip-tube. The oil-refrigerant mixture then is cooled in the oil cooler and throttled through a set of metering valves in order to control the oil injection mass flow rate. The flow rate of injected oil is measured with a Coriolis-type flow meter.

2.1. Compressor

The compressor utilized for the experimental testing with oil injection is an experimental R410A scroll air-conditioning compressor that included injection ports added to a conventional compressor. Figure 4 shows the compressor installed in the system. The injection ports are located such that they open to the compression chambers just after the compression pockets have been sealed off from the suction chambers. The product information for the compressor gives a displacement rate of 5.8 m^3 h^{-1} at 3500 RPM, or a displacement per rotation of 27.6 cm^3.

This compressor is designed for air-conditioning applications, and as a result has a decrease in efficiency at lower evaporating temperatures due to a relatively low volume ratio for the imposed pressure ratio, among other design considerations. The compressor runs on a 220 V single-phase supply and rotates at 3500 RPM under load.

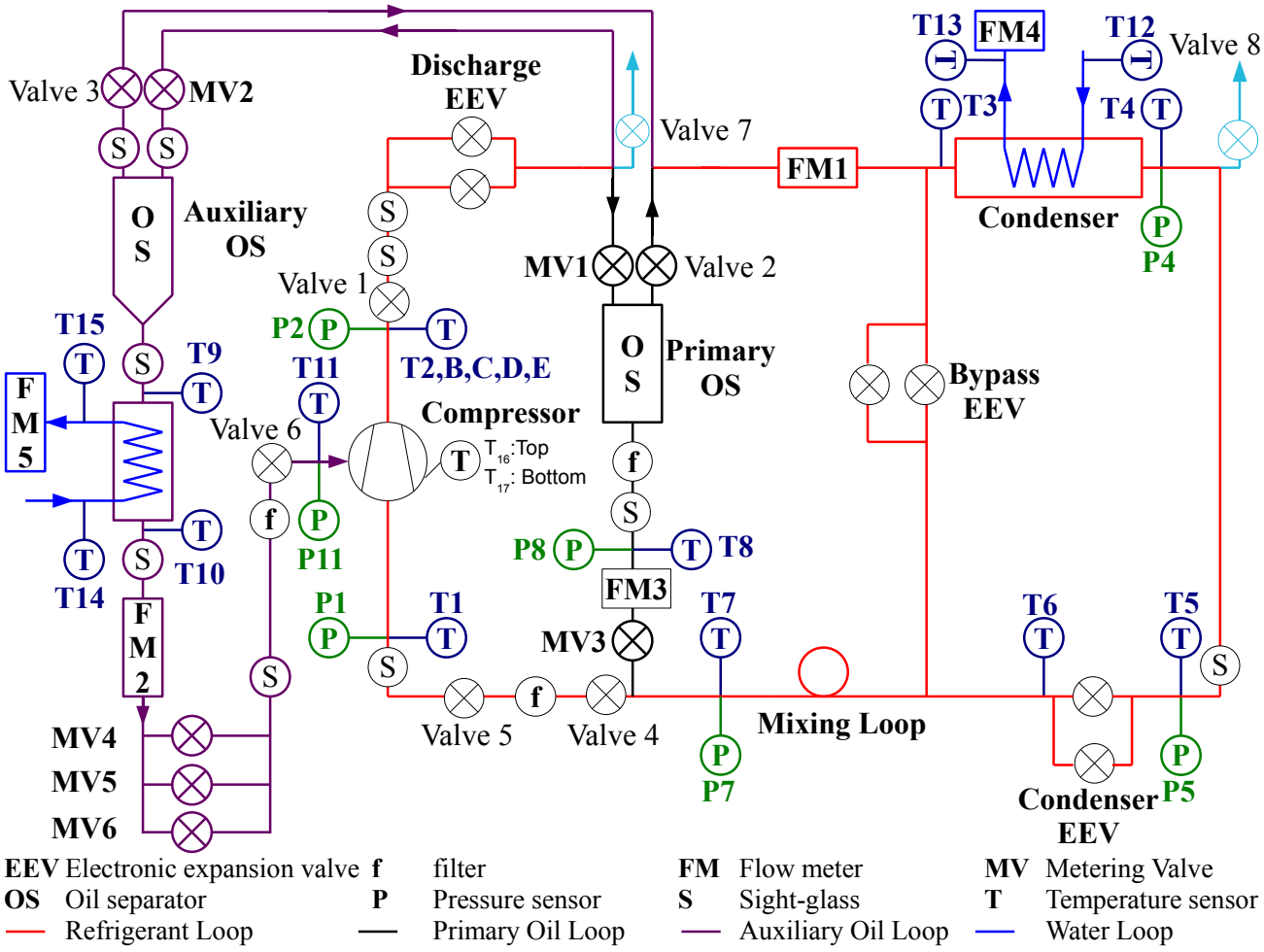

Figure 3: Schematic of oil-flooded hot gas bypass stand

The compressor was further modified in order to be able to readily measure the oil level in the sump of the compressor. A small hole was drilled in the bottom of the compressor shell at the dead center location, and this tap was connected to a sight glass in parallel with the compressor. The top of the sight glass was connected to the suction line to equalize the pressure in the sight glass since the compressor was a low-pressure shell type compressor. Therefore the oil levels in the sight glass and the compressor shell should have been equal.

The oil employed in this experimental testing program is a polyol-ester (POE) oil. The manufacturer recommends this oil for this compressor when operating with refrigerant R410A.

2.2. Measurement Devices

The temperatures at all points in the system were measured with Omega T-Type sheathed thermocouples fully inserted in the flow. All the thermocouples were checked against two reference temperatures - the freezing point and boiling point of distilled water at ambient pressure. All of the thermocouples agreed with the reference temperatures to within 0.2°C.

At the discharge of the compressor it was thought initially that there might be significant thermal non-equilibrium effects based on the thermal non-equilibrium challenges experienced in the Liquid-Flooded Ericsson Cycle testing described in Bell (2011). For that reason, a five-thermocouple system was installed at the discharge of the compressor in the hopes of capturing any thermal non-equilibrium effects if they were present. Two thermocouples were surface mounted on the tube outer wall, and three were installed in the flow, with one pointed upwards and one pointed downwards. The surface mounted thermocouples were wrapped with approximately 1 cm of insulation after installation. Analysis of the experimental data suggests that good thermal equilibrium between the oil and refrigerant phases is achieved at the outlet of the compressor due to the highly turbulent flow in the com-

pression process.

Furthermore, two thermocouples were installed on the shell of the compressor to obtain an accurate shell temperature. One thermocouple was installed on the body of the compressor shell, and the other thermocouple was installed on the top of the compressor shell, dead-center.

The pressure transducers were calibrated against a reference pressure transducer with accuracy of 3.44 kPa. After calibration, all the pressure transducers were within tolerance of the reference transducer.

The refrigerant mass flow rate was measured with a Coriolis mass flow meter with accuracy of 0.35% and full scale range of 1888 g s^{-1}. The oil injection flow rate was also measured with a Coriolis flow meter with full scale range of 605.5 g s^{-1} and accuracy of 0.05% for flow rates above 30.275 g s^{-1}, and an absolute accuracy of 1.513x10-2 g s^{-1} below 0.030275 kg s^{-1} (5% of full scale). The oil injection flow meter can also measure the density with an accuracy of 0.2 kg m^{-3}. The condenser water flow was measured with a Coriolis mass flow meter with full scale range of 755 g s^{-1} and accuracy of 0.5%. The oil cooler water flow rate was measured with a Coriolis flow meter with full scale range of 188.8 g s^{-1} and accuracy of 0.15%. The oil return mass flow rate was measured with a gear-type flow meter with maximum capacity of 13.2 U.S. gallons per hour.

The electrical power of the compressor was measured with a Scientific Columbus model XL-525-A2 power meter with accuracy of 0.2% of the reading.

3. Experimental Testing

3.1. Solubility

In the oil separators, oil and the refrigerant come to a thermodynamic equilibrium, the result of which is that some amount of refrigerant remains dissolved in the oil. In general, the solubility mass fraction is a function of both temperature and pressure. Data for the solubility of R410A in the POE oil can be found in Bell (2011). For a given temperature, as the pressure increases, the amount of refrigerant dissolved in the oil increases. For a given pressure, as the temperature increases, the amount of refrigerant dissolved in the oil decreases. Using the measured pressure and temperature in the oil injection oil separator it is therefore possible to estimate the mass fraction of refrigerant dissolved in the oil (X_{sep}). The pressure of the oil within the separator was assumed to be equal to the intermediate pressure measured at the inlet of the condenser. The net result was that a R410A mass fraction of approximately 0.15 was dissolved in the oil at the outlet of the separator and subsequently re-injected into the compressor through the oil injection port.

3.2. Calculations

The dew temperatures for the compressor are found from the measured suction and discharge pressures. Then the compressor inlet superheat is defined as

$$\Delta T_{sh} = T_1 - T_{dew,s} \tag{1}$$

The mass flow rates of refrigerant ($\dot{m}_{ref}$) and oil with dissolved refrigerant ($\dot{m}_l$) are directly measured and thus the liquid mass fraction can be given by

$$x_l = \frac{\dot{m}_{\text{ref}}}{\dot{m}_{\text{ref}} + \dot{m}_l} \tag{2}$$

The total isentropic power is given by the sum of the isentropic power required to compress the suction refrigerant to the discharge pressure and the power needed to isentropically compress the injected mixture of oil and refrigerant oil to the discharge pressure or

$$\dot{W}_i = \dot{m}_{\text{ref}}(h_{2s} - h_1) + \dot{m}_l(h_{2s,inj} - h_{11}) \tag{3}$$

where h_{2s} and $h_{2s,inj}$ are the isentropic compression enthalpies from the suction and injection pressures respectively to the discharge pressure. The injected mixture is modeled based on homogeneous oil-refrigerant mixture properties as described in Bell (2011). Therefore the overall isentropic efficiency can be given by

$$\eta_{oi} = \frac{\dot{W}_i}{\dot{W}_{\text{el}}} \tag{4}$$

As in the analysis for the Liquid-Flooded Ericsson Cycle testing presented in Bell (2011), the uncertainties of all the derived parameters were calculated based on an automatic uncertainty calculation routine. All the data reduction calculations were embedded in an outer loop that calculated the uncertainties of each parameter by numerical differentiation. Thus the calculations can be freely modified or other output parameters can be calculated, and the experimental uncertainties will be automatically updated.

3.3. Test Matrix

To develop an understanding of the performance of the compressor with oil flooding, the compressor was run at a selection of test points. Since the motivation for this set of experimental testing is to apply liquid-flooding and regeneration to low-temperature heat pumping applications, low evaporation temperatures were employed. The goal was to test the compressor down to suction dew temperatures as low as -20°C. Unfortunately refrigerant flow instabilities at suction dew temperatures lower than -10°C made it impossible to achieve a stable superheat at a suction dew temperature of -20°C. Altering the valve C_v by less than 0.0001 resulted in a change in superheat of 0.3°C. It would seem that at a suction dew temperature of -20°C, the two-phase flow in the condenser was on the cusp of transition between flow regimes, as it was possible to hear different flow patterns with the use of a screwdriver applied to the tube at the outlet of the condenser valves. At higher evaporation temperatures, oil management became difficult because the higher flow rates of refrigerant through the compressor resulted in larger amounts of oil entrainment in

the refrigerant passing through the compressor shell. As a result, the compressor sump needed to be refilled so frequently that it was impossible to achieve steady-state operation at higher suction dew temperatures. As a result, the only suction dew temperature that could be used in this configuration was -10°C.

The configurations shown in Table 1 were used to test the compressor. For configurations A through D, the oil flow rate was varied in order to yield nominal increments in the oil mass fraction of 0.05. The highest mass fraction in each set was the maximum amount of oil that could be injected in the compressor with all the oil injection valves fully open. At the highest oil mass flow rates, there was up to a 2 bar pressure difference between the system intermediate pressure and the injection port pressure. The superheat was set at 11.1 K for consistency with the rating data for the compressor. In practice, in the liquid-flooded application, the superheat will be much higher, and the inlet temperature to the compressor will be near the heat sink temperature due to regeneration. The tested compressor could not operate at the very high superheat states because it was impossible to inject enough oil to keep the discharge temperature sufficiently low. Configuration E was meant to try to understand the performance of the compressor at higher superheat. Table 2 presents the results of the compressor for the 35 data points presented here. Further results are available in Bell (2011).

At each state point, at least 5 minutes of steady-state data was acquired. The condensing and evaporating pressures were very stable because they were being dynamically controlled with PID controllers, while the superheat tended to vary because of slight variations in the inlet water temperature to the condenser. The data was then post-processed to calculate all parameters not directly calculated and the uncertainties of all parameters. The pertinent parts of the analyses can be found in the appendices of Bell (2011).

4. Experimental Results

Figure 5 shows the performance of the compressor at the -10°C suction dew temperature / 30°C discharge dew temperature configuration (configuration A). The manufacturer data for the compressor at this state point without injection ports yields an isentropic efficiency of 66.4%, electrical power of 1650 W and refrigerant mass flow rate of 31.2 g s^{-1}.

When no oil injection is used (x_l=0), the compressor performance is worse than the manufacturer rating data for the compressor. This decrease in performance is due to the re-expansion losses of the gas in the oil injection lines. During each rotation of the compressor the gas in the oil injection lines is compressed, and then subsequently re-expands, causing irreversibilities. The irreversibilities are manifest as a heating source term, which result in a higher discharge temperature, and less mass flow rate due to suction gas heating. In addition, due to a few adverse lubrication events when the oil sump ran out of oil during the oil refilling process, some mechanical damage would seem to have been done to the compressor.

Once even a small amount of oil injection is introduced, the mass flow rate jumps back to the rating mass flow rate. This is due to the fact that as soon as there is some flow of oil in the injection lines, they are then full of incompressible oil rather than compressible refrigerant vapor, and the re-expansion losses from the injection lines are eliminated. The power does not fully recover to the rating data, largely due to the mechanical damage caused by the adverse lubrication events. As the oil injection rate is increased, the refrigerant mass flow rate increases slightly. This increase in refrigerant mass flow rate occurs due to a decrease in heat transfer to the gas in the suction pocket because the rest of the compression process is more isothermal.

As increasing amounts of oil are injected, the refrigerant mass flow rates continue to increase. The discharge temperature of the compressor decreases monotonically with larger oil mass fractions due to the refrigerant's heat of compression being transferred to the oil. The mechanical power remains effectively constant until an oil mass fraction of 0.30. Between an oil mass fraction of 0.25 and 0.30 there is a step change in the electrical power. This same effect is seen in the other tests described below. The physical mechanism behind this increase in power is not clear, but it has been surmised that it might be due to a dis-engagement of the radial compliance mechanism due to large oil film forces, or a transition in flow regime resulting in a large change in discharge pressure drops. Or the increase in power could be a result of a disturbance in the lubrication of the compression mechanism, even though there was a sufficient amount of oil in the compressor sump. The introduction of two-phase flow effects makes analysis of the compression process and all the physical phenomena that contribute to the electrical power more difficult.

As oil is injected into the compression process, the overall isentropic efficiency of the compressor generally increases monotonically with increasing amounts of oil injection. The only exception is between oil injection mass fractions of 0.25 and 0.3, where there is a small step in the overall isentropic efficiency due to the discontinuity in the electrical power. Overall, the efficiency at the higher mass fractions significantly exceeds the rated efficiency for the un-flooded compressor.

At a discharge dew temperature of 43.3°C (configurations B through D), the performance of the compressor with oil injection is qualitatively similar to the performance at a discharge dew temperature of 30°C. Figure 6 shows the results for the compressor with varying amounts of oil injection, as well as varying the amount of cooling of the oil prior to injection. The nominal rating for the compressor at this state point is an electrical power of 2290 W, overall isentropic efficiency of 0.596, and refrigerant mass flow rate of 29.6 g s^{-1}.

When the oil is not actively cooled prior to injecting

Table 1: R410A Test Matrix

Config	$T_{dew,s}$ [°C]	$T_{dew,d}$ [°C]	ΔT_{sh} [K]	Oil
A	-10	30	11.1±0.1	Cooled to 25±3°C
B	-10	43.3	11.1±0.1	Not Cooled
C	-10	43.3	11.1±0.1	Cooled to 35°C
D	-10	43.3	11.1±0.1	Cooled to 15°C
E	-10	43.3	11.1±0.1,25±0.1	Cooled to 35°C, x_l=0.3

Table 2: Experimental data from the testing of R410A scroll compressor with oil injection.

#	T_1 °C	T_2 °C	T_{11} °C	T_{amb} °C	p_1 kPa	p_2 kPa	p_{11} kPa	$T_{dew,s}$ °C	$T_{dew,d}$ °C	ΔT_{sh} K	x_l -	$\dot{m}_{ref}$ g s^{-1}	$\dot{m}_l$ g s^{-1}	$\dot{W}_{\text{el}}$ kW	η_{oi} -
1	1.0	81.2	23.9	24.0	573	1885	669	-10.0	30.0	11.0	0.000	30.08	-0.09	1.781	0.597
2	1.2	73.4	26.2	23.8	574	1882	677	-9.9	30.0	11.1	0.049	31.37	1.63	1.727	0.645
3	1.1	69.9	26.5	24.3	573	1884	694	-10.0	30.0	11.2	0.097	31.32	3.37	1.727	0.651
4	1.0	66.0	26.5	24.1	571	1875	720	-10.1	29.8	11.0	0.151	31.34	5.57	1.721	0.658
5	1.0	63.5	26.9	24.3	573	1880	743	-10.0	29.9	11.0	0.197	31.45	7.70	1.725	0.664
6	1.0	60.3	26.6	24.0	573	1885	737	-10.0	30.0	11.0	0.254	31.57	10.76	1.731	0.675
7	1.1	58.2	26.7	24.2	573	1887	742	-10.0	30.1	11.1	0.305	31.55	13.85	1.759	0.674
8	1.1	56.2	27.1	24.0	573	1884	765	-10.0	30.0	11.1	0.350	31.57	17.00	1.758	0.683
9	0.9	53.9	27.1	24.4	571	1877	804	-10.1	29.9	11.0	0.399	31.55	20.98	1.753	0.693
10	1.1	52.8	27.3	24.3	573	1881	823	-10.0	29.9	11.1	0.430	31.66	23.92	1.760	0.700
11	1.2	116.4	26.3	24.6	574	2620	836	-9.9	43.3	11.1	0.000	26.34	-0.09	2.402	0.500
12	1.1	99.6	32.8	26.2	573	2619	684	-10.0	43.3	11.1	0.051	29.62	1.60	2.305	0.592
13	0.9	94.6	44.2	25.4	573	2615	726	-10.0	43.2	10.9	0.106	29.94	3.56	2.293	0.605
14	1.1	93.2	50.6	25.4	573	2619	774	-10.0	43.3	11.0	0.153	29.76	5.37	2.308	0.603
15	1.1	91.8	54.8	25.6	573	2620	810	-10.0	43.3	11.1	0.196	29.72	7.25	2.311	0.606
16	1.2	90.3	58.9	25.9	572	2615	839	-10.0	43.2	11.2	0.251	29.77	9.96	2.310	0.613
17	1.3	89.4	61.4	26.1	575	2625	859	-9.9	43.4	11.2	0.300	29.88	12.82	2.349	0.611
18	1.0	88.8	63.5	26.6	571	2615	871	-10.1	43.2	11.1	0.349	29.70	15.89	2.357	0.613
19	1.4	88.0	65.6	26.7	574	2614	890	-9.9	43.2	11.3	0.396	29.86	19.62	2.360	0.622
20	1.1	87.5	67.2	26.7	572	2616	903	-10.0	43.3	11.2	0.448	29.71	24.09	2.369	0.628
21	1.1	74.3	34.8	27.8	571	2617	814	-10.1	43.3	11.2	0.363	30.39	17.35	2.312	0.646
22	1.2	78.2	34.9	28.0	573	2620	778	-10.0	43.3	11.2	0.301	30.44	13.14	2.317	0.634
23	1.2	81.8	35.0	28.1	573	2619	806	-10.0	43.3	11.1	0.248	30.41	10.01	2.314	0.625
24	1.0	85.4	34.8	28.1	571	2618	781	-10.1	43.3	11.1	0.200	30.20	7.55	2.314	0.616
25	1.2	89.9	35.0	28.4	573	2619	763	-10.0	43.3	11.2	0.148	30.11	5.21	2.309	0.609
26	1.1	94.2	34.9	28.8	572	2619	734	-10.0	43.3	11.1	0.100	29.96	3.33	2.308	0.602
27	4.9	80.2	35.0	27.3	573	2617	834	-10.0	43.3	14.9	0.299	29.96	12.75	2.314	0.634
28	15.1	85.4	35.0	26.7	572	2618	826	-10.0	43.3	25.1	0.302	28.66	12.40	2.329	0.635
29	1.2	111.2	26.4	26.6	571	2615	695	-10.1	43.2	11.3	0.000	27.99	-0.09	2.353	0.545
30	1.1	97.4	18.1	22.4	572	2620	726	-10.0	43.3	11.1	0.050	29.78	1.58	2.293	0.598
31	1.4	90.4	15.8	24.3	575	2619	751	-9.9	43.3	11.2	0.103	30.28	3.47	2.298	0.608
32	1.1	85.1	15.5	25.3	572	2616	773	-10.0	43.3	11.1	0.151	30.22	5.38	2.300	0.611
33	1.1	79.6	15.3	23.0	572	2617	795	-10.0	43.3	11.1	0.201	30.45	7.64	2.304	0.618
34	1.1	75.2	15.4	22.5	572	2617	813	-10.0	43.3	11.1	0.250	30.61	10.20	2.318	0.622
35	1.1	69.4	16.0	20.9	573	2620	846	-10.0	43.3	11.1	0.323	30.83	14.68	2.314	0.638

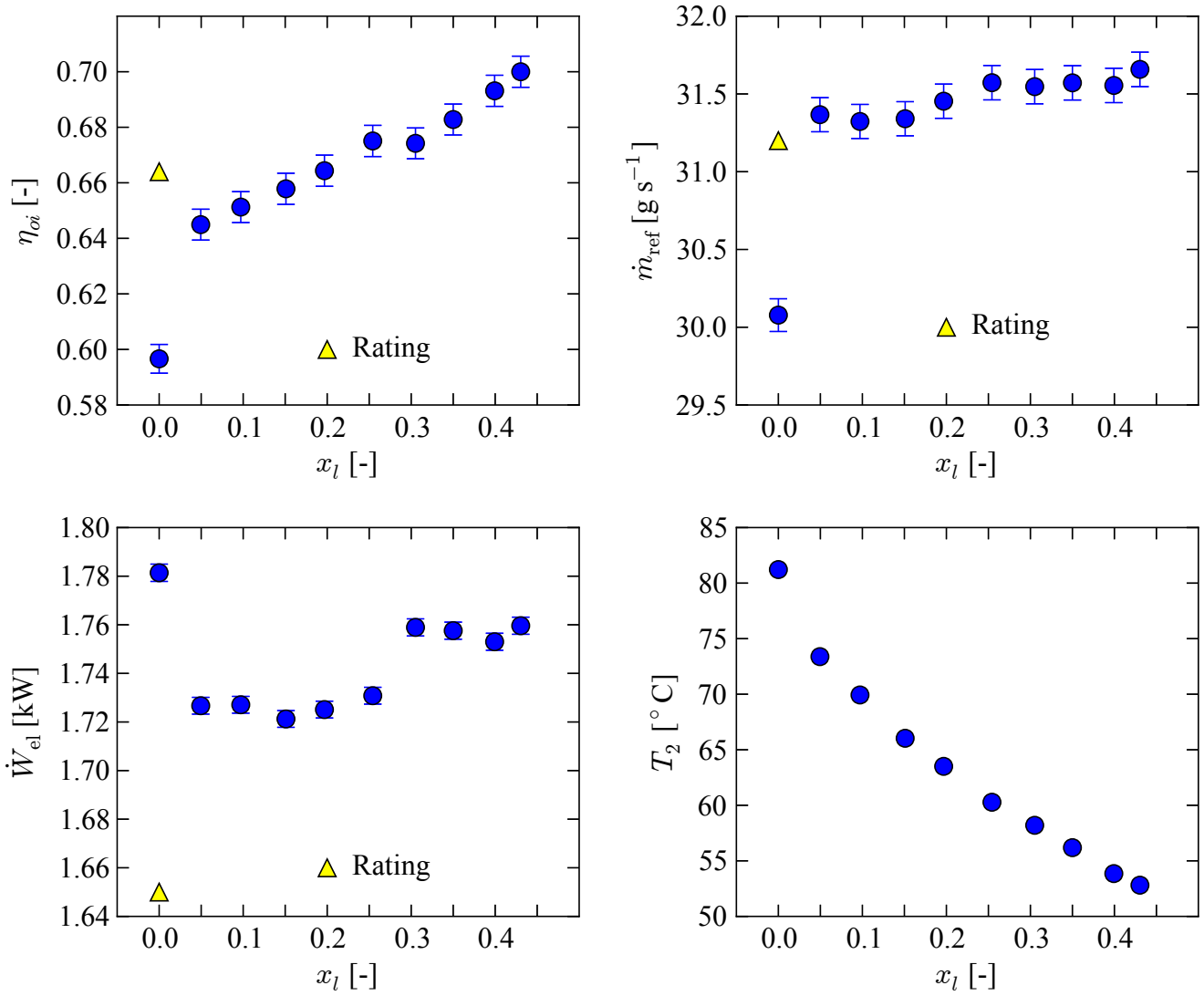

Figure 5: Performance of oil-injected compressor for $T_{dew,s}$=-10°C and $T_{dew,d}$=30°C with and without oil injection (Error bars: uncertainty).

it into the compressor, the oil is not as able to provide cooling of the refrigerant during the working process - in fact the injected oil is much hotter than the fluid in the compression pocket when it comes into contact with the injected oil. As a result, the discharge temperature of the compressor sees only a small decrease from the oil injection. The refrigerant mass flow rate is effectively constant. Again, the sharp step change in electrical power between oil mass fractions of 0.25 and 0.3 is experienced.

When the oil is cooled to 35°C prior to injection into the compressor, the refrigerant mass flow rate increases due to the cooler inlet temperature of the oil. The discharge temperature of the compressor sees a large decrease in temperature from 111.2°C without oil injection to 74.3°C at an oil mass fraction of 0.363. This testing condition simulates cooling the oil against the sink temperature for an air-to-air heat pump application where the sink temperature is the interior of the building to be heated.

Further cooling the oil to an injection temperature of 15°C, the benefits to compressor performance are increased. There is a slight improvement in the refrigerant mass flow rate compared to the 35°C oil injection temperature, but the primary influence is on the discharge temperature of the compressor, which is decreased down to 69.4°C. This condition was designed to simulate cooling the oil against the outdoor temperature, though colder temperatures could not be achieved since the oil cannot be cooled below the cold water inlet temperature.

At both oil injection temperatures of 15°C and 35°C, the overall isentropic efficiency increases monotonically with an increase in oil injection mass fraction. When the oil is not cooled, the overall isentropic efficiency also increases monotonically with the oil injection mass fraction but at a slower rate and with the exception of the same disconti-

nuity between oil injection mass fractions of 0.25 and 0.30. The discontinuity in the overall isentropic efficiency without oil cooling is due to the discontinuity in the electrical power.

Figure 7 shows the performance of the compressor with an oil injection mass ratio of 0.30 for varied suction superheat. As the superheat is increased, the refrigerant mass flow rate decreases due to the decrease in refrigerant density at higher superheat. Thus when designing a compressor for practical application to oil flooding with regeneration systems, larger compressor displacements would be needed for the same system heating or cooling capacity due to the extremely high superheat. The discharge temperature of the compressor also increases due to the higher suction temperature, but the increase in discharge temperature is less than the increase in suction superheat. The overall isentropic efficiency is constant to within the experimental uncertainty.

5. Conclusions

An air-conditioning compressor for refrigerant R410A with a vapor-injection port has been tested with oil injection. The compressor was installed in a well-instrumented testing facility in order to measure performance with oil injection. It was found that in general the injection of oil results in an increase in refrigerant mass flow rate and overall isentropic efficiency and a decrease in the compressor discharge temperature. This dataset suggests that designing an efficient compressor with oil injection for application to a low-source-temperature air-source heat pump application should be possible. As a result, oil-flooded vapor compression systems should perform even better than the conservative assumption of constant efficiency employed in the simplified cycle analysis from Bell et al. (2011).

6. Acknowledgements

The work in this paper is adapted from the Purdue University PhD. Thesis entitled Theoretical and Experimental Analysis of Liquid Flooded Compression in Scroll Compressors by Ian Bell, published in 2011. Full-text: http://docs.lib.purdue.edu/herrick/2/

7. References

Blaise, J. and T. Dutto., 1988, Influence of oil injection and pressure ratio on single screw performances at high temperatures. In 1988 International Compressor Engineering Conference at Purdue University, pages 338-345

Bell, I., Groll, E., Braun, J., King, G., Horton, W.T., 2011, Performance of Vapor Compression Systems with Compressor Oil Flooding and Regeneration. Int. J. Refrig. v. 34 n. 1. doi:10.1016/j.ijrefrig.2010.09.004

Bell, I., 2011. Theoretical and Experimental Analysis of Liquid Flooded Compression in Scroll Compressors. Ph.D. thesis, Purdue University. http://docs.lib.purdue.edu/herrick/2/

Hiwata, A., N. Iida, Y. Futagami, K. Sawai, and N. Ishii., 2002, Performance investigation with oil-injection to compression chambers on CO_2-scroll compressor. In 2002 International Compressor Engineering Conference at Purdue University, number C18-4.

Kemp G., Elwood, L. and E. A. Groll. 2010, Evaluation of a Prototype Rotating Spool Compressor in Liquid Flooded Operation. In 20th International Compressor Engineering Conference at Purdue University, 2010.

Stosic, N. , L. Milutinovic, K. Hanjalic, and A. Kovacevic., 1990, Experimental investigation of the influence of oil injection upon the screw compressor working process. In 1990 International Compressor Engineering Conference at Purdue University, pages 34-43.

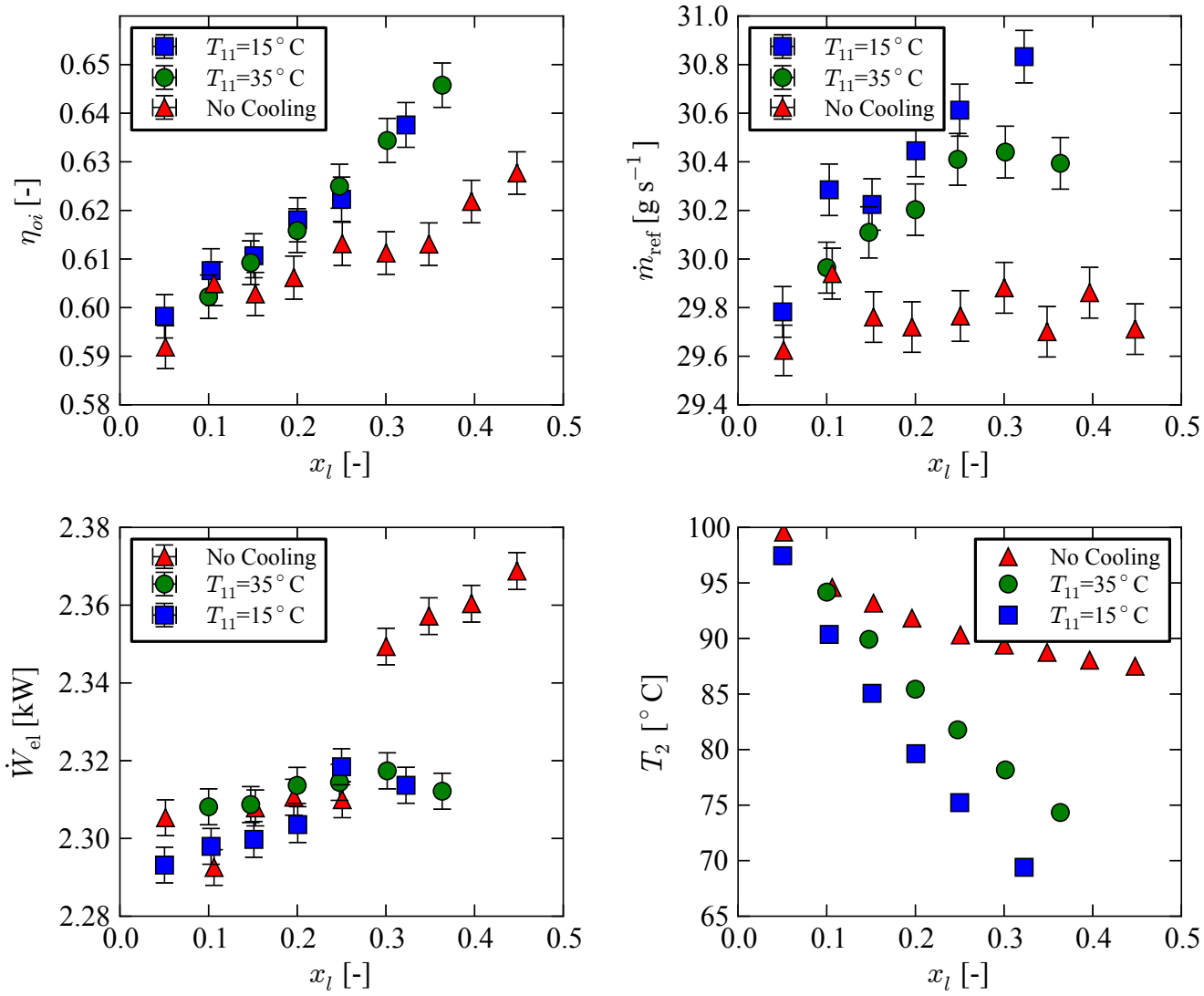

Figure 6: Performance of oil-injected compressor for $T_{dew,s}$=-10°C and $T_{dew,d}$=43.3°C with and without oil injection (Error bars: uncertainty)

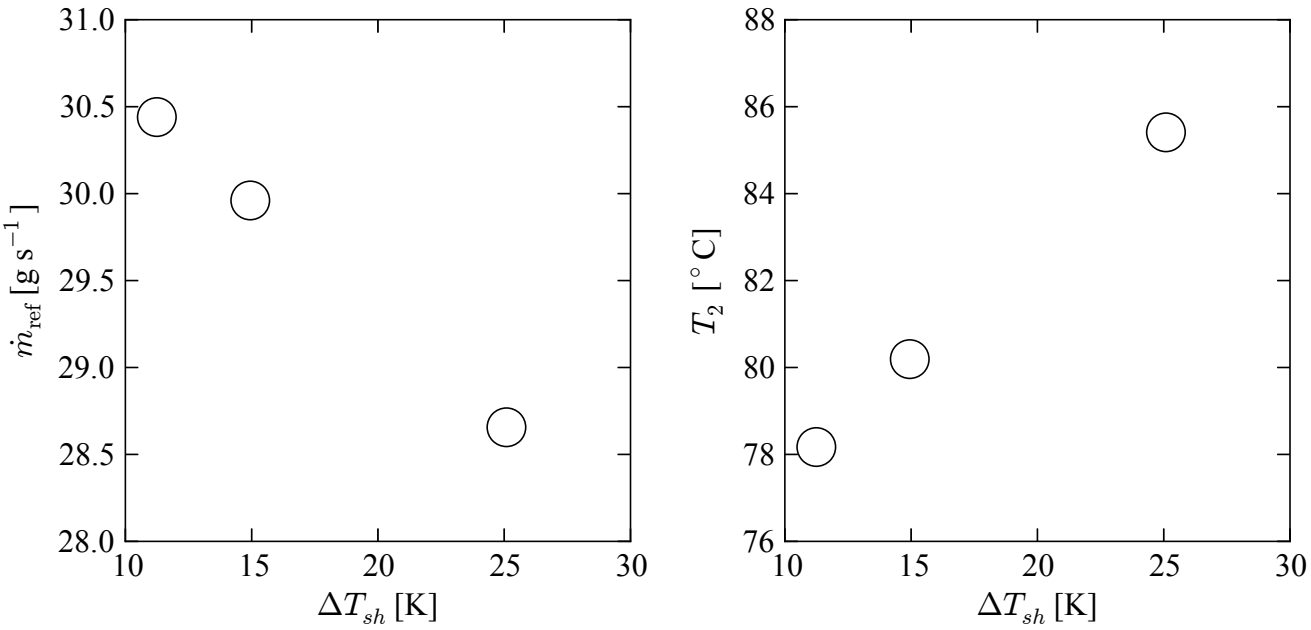

Figure 7: Performance of compressor for varied superheat ($T_{dew,s}$=-10°C, $T_{dew,d}$=43.3°C, x_l=0.30, T_{11}=35°C)